Incremental sequentially linear analysis to control failure for quasi-brittle materials and structures including non-proportional loading

Yu, Chenjie; Hoogenboom, P. C.J.; Rots, J. G.

DOI
10.1016/j.engfracmech.2018.07.036

Publication date
2018

Document Version
Accepted author manuscript

Published in
Engineering Fracture Mechanics

Symbols and Abbreviations

Roman symbols

f_t	Tensile strength
G_f	Mode-I tensile fracture energy
h	Crack band width
K	Current stiffness matrix
q	Load reduction factor in ISLA
r	Convergence tolerance of μ in ISLA
t	Stiffness reduction factor
v	Initial load factor for non-proportional loading in SLA

Greek symbols

ε_u	Ultimate tensile strain
λ	Load factor in SLA
μ	Utilisation function which is the largest utilization value of all elements in ISLA

Abbreviations

CITA	Continuous incremental-only tangential analysis
IMPL−EX	Implicit-explicit approach
ISLA	Incremental sequentially linear analysis
LATIN	The large time increment method
NIEM	Non-iterative energy based method
NR	Newton–Raphson method
SLA	Sequentially linear analysis
SUR	Smooth unloading-reloading function approach

Incremental Sequentially Linear Analysis to Control Failure for Quasi-brittle Materials and Structures including Non-proportional Loading

Chenjie Yu, P.C.J. Hoogenboom, J.G. Rots,
Delft University of Technology, Delft, the Netherlands

Abstract
Quasi brittle materials, such as un-reinforced masonry or concrete are difficult to analyse because often the traditional Newton – Raphson (N-R) procedure fails to converge. Many solutions have been proposed such as Sequentially Linear Analysis (SLA), but these may fail in case of non-proportional loading with a large prestress. In this paper a new method is proposed that is based on a combination of the Newton – Raphson method and Sequentially Linear Analysis. The method is incremental; each increment starts and ends with an equilibrium state. The solution search path follows damage cycles sequentially with secant stiffness. The proposed method is demonstrated to be robust and accurate. It has been tested on prestressed concrete beams. It can be naturally extended to other types of analyses (e.g. geometrically non-linear analysis and transient analysis) due to the incremental procedure. In addition, it is shown that high prestress values can transform the behaviour of a concrete beam from softening to hardening.

Keywords: Structural analysis, incremental, iterative, implicit, explicit, sequentially linear analysis (SLA), Newton-Raphson (N-R) method, masonry, unreinforced concrete

1. Introduction

Nonlinear analysis of quasi brittle materials, such as masonry, concrete, reinforced and prestressed concrete, has been applied for more than 40 years. However, the robustness of the algorithms is still a serious issue. The load-displacement curves of quasi brittle materials have many little peaks related to initiation and propagation of numerous cracks. These peaks are only visible if one zooms in on a curve which is computed with very small load increments. Consequently, the tangent stiffness in the neighbourhood of these peaks varies extremely and can lead to divergence of the Newton-Raphson (N-R) iterations in certain displacements.

Many solution methods have been proposed to adapt the full N-R method (e.g. [1]) or introduce new approaches of solving non-linear problems. The modified N-R method computes and decomposes the tangential stiffness matrix only in the first iteration at the beginning of every load step while the full N-R method sets up and decomposes the tangent stiffness matrix in every iteration. The global tangent stiffness in the N-R method can be based on true negative softening stiffness at local level or on the positive secant stiffness at local level. Also, arc-length schemes can be added, which is a modification of load control in order to trace post-failure behavior numerically when a structure softens or snaps back [2][3][4][5]. However, these techniques cannot prevent divergence or ill-conditioning of the system of equations in case of brittle behaviour. A new constraint has been developed based on the energy release rate in term of geometrically linear damage, geometrically linear plasticity and geometrically non-linear damage to improve the robustness of the arc length method in [6]. In the implicit–explicit approach (IMPL-EX), the explicit (non-iterative) scheme and implicit (iterative) scheme are combined [7][8]. IMPL-EX combines an implicit scheme of the stresses in the constitutive model with an explicit extrapolation of the involved

internal variables. The length of the time step influences the accuracy of this method [9]. The LATIN method is a non-incremental iterative computational strategy applied over the entire time interval [10]. The main features are the separation of possibly non-linear local equations in space and time and possibly global linear equations in the spatial variable, a two-step iterative approach and an ad-hoc space-time global approximation. The difficulty is to define the search paths in the two-step scheme, which currently is guided by numerical parameters that do not have a clear physical meaning. A fictitious viscosity has been added in the constitutive equations for the cohesive interface to trace the instable post-behaviour [11].

In order to enhance the robustness of solving non-linear problems, a total approach with secant stiffness (Load-Unload method) and an "event-by-event" damage model (saw tooth constitutive law) has been introduced by sequentially linear analysis [12]. Sequentially linear analysis (SLA) is an alternative to the Newton-Raphson method when bifurcation, snap-back or divergence problems arise. The incremental-iterative procedure, adopted in nonlinear finite element analysis, is replaced by a sequence of scaled linear finite element analyses with decreasing secant stiffness, corresponding to local damage increments [13]. The saw tooth model has been improved in [13][14] to make the results independent of the magnitude of the stiffness reduction in a step. The SLA with fixed smeared cracking has been improved with a damage dependent shear modulus decreasing along with Young's modulus to reduce the mesh-directional bias for fixed smeared cracking [15]. Two methods are proposed to perform SLA with non-proportional loading [16][17]. An algorithm selects the critical integration point to which a damage increment is applied by extra stresses [16] or a varying constant-load factor [17]. The non-proportional loading method in [16] has been improved by a constrained optimization to suit for more non-proportional loading cases [18]. Non-proportional loading still has limitations; the method fails when a large initial overburden force is applied [19]. In addition, Coulomb friction laws have been introduced for tension-shear failure criterion [18]. SLA has similarity to the discretized lattice model method [20] [21] [22]. In lattice models, the continuum is replaced by a lattice of truss or beam elements. Therefore, the micro structure of the material can be simulated by assigning different properties. A truss or beam element is removed when a failure criterion is reached in a brittle material.

In addition to developing total approaches, research is also ongoing to improve the robustness and efficiency of incremental approaches. The predictive SUR approach [23] uses a smooth unloading-reloading function (SUR) to compute an approximate tangent stiffness matrix, which is used in a non-linear incremental-iterative N-R method. The predictive SUR approach is more efficient than the secant method, but the form of the SUR function significantly affects the convergence characteristics of the model. The strong discontinuity approaches [24] define in each increment either a loading phase or an unloading phase with the crack state frozen to improve the robustness when a sudden propagation of cracks through several elements occurs in one increment. Each time when a crack segment is added in an element, an unloading phase with frozen crack propagation is performed. If the propagation criterion is met simultaneously in more than one element, the crack is added in the critical element. Other improved approaches are Non-iterative energy based method (NIEM) [25] and Continuous incremental-only tangential analysis (CITA) [26], both of which adopt piecewise linear continuum laws. NIEM uses tangent stiffness to scale the global load increments according to the local discontinuity in the multi-linear stress-strain diagram. NIEM allows for switching between the incremental and the total approach based on energy dissipation. When a critical bifurcation point is reached, it is impossible to incrementally determine the effective path and the switch to a total method is adopted with the secant

material stiffness. When NIEM switches to the total approach, the non-proportional loading issue remains. CITA is presented as a continuous, incremental-only, tangential analysis for the Newton – Raphson method. Again, the tangent elasticity modulus is based on the true negative stiffness. This method improves the efficiency compared with the secant method and keeps track of the displacement history. The CITA method attempts to control energy dissipation by limiting the damage level to a single event. Negative tangent stiffness may still cause divergence problems, e.g. in case of snap-backs. The Force-Release method [27] extends saw-tooth constitutive laws to an incremental and non-iterative procedure. The Force-Release method is based on redistribution of released stresses. It preserves the linearity of each step. After rupture of the critical element, a sequentially linear redistribution process of stress release takes place until a static equilibrium state is reached. However, the method does not follow snap-backs. In an attempt to follow snap-backs, the Force-Release method is combined with the Load-Unload method [28]. The result is a range of possible solutions, which depends on the choice of external load velocity and ratio between disequilibrium forces and external load increment.

In this paper a new method is proposed which combines the advantages of the Newton – Raphson method and Sequentially Linear Analysis. The new method will be demonstrated to work effectively for non-proportional problems but it can be naturally extended to include geometrical nonlinearity, plasticity for cyclic loading and transient analysis.

The idea behind the proposed method is to perform an incremental analysis with Newton-Raphson iterations and linear elastic material behaviour with load or displacement control. As soon as the stress somewhere is too large, the Young's modulus of the considered element is reduced and the load is reduced or increased to the level at which the stress is just not too large. The method is robust because all physical nonlinearity is included in stiffness damage cycles.

2. General equations and procedures of the new algorithm

Suppose that a structure is loaded by two load cases, one with a constant load factor λ_1 and the second with a varying load factor λ_2. This is referred to as non-proportional loading. Here λ_2 can be incremented (2.1 Load control) or first incremented and then automatically decremented (2.2 "Arc length" control). In proportional loading, on the other hand, there is only λ_2 and no λ_1.

Just as in SLA, utilisation values are computed for each element. A utilisation function μ is defined as the largest utilisation value of all elements, which is a function of the load factors and the stiffness matrix K. The material is in equilibrium if

$$\mu(\lambda_1, \lambda_2, K) \leq 1, \tag{1}$$

which means that the stresses or strains of the critical element, i.e. the element that is most close to a first or next damage moment, lie either on or within the failure surface.

2.1 Load control

For the load control, λ_1 is fixed for all load steps and λ_2 is incremented. Note that λ_2 is fixed within a load step. The load factor λ_2 is applied to imposed forces or imposed displacements. Suppose that after load step *n* somewhere the failure surface is reached.

$$\mu_n = \mu(\lambda_1, \lambda_2, K_n) = 1 \tag{2}$$

where the subscript on μ and *K* refer to a load step.

For the next step λ_2 is increased to λ_2'. If

$$\mu_{n+1}^1 = \mu(\lambda_1, \lambda_2', K_{n+1}^0) > 1 \tag{3}$$

where $K_{n+1}^0 = K_n$

then restart from μ_n, which means that the displacements are reset to the values at the end of step *n*. Subsequently the stiffness matrix is reduced.

$$\mu_{n+1}^2 = \mu(\lambda_1, \lambda_2', K_{n+1}^1) \tag{4}$$

where K_{n+1}^1 means that the Young's modulus of the critical finite element is reduced in the stiffness matrix for this step, which is based on the rotating smeared crack with constant stiffness reduction *t*. In this model, the Young's modulus in principal directions of the critical finite element is reduced. A step in which the stiffness is reduced is called a cycle. The superscripts on μ and *K* refer to the cycle number of a load step.

Restart from μ_n and continue reducing the stiffness matrix until

$$\mu_{n+1}^{m+1} = \mu(\lambda_1, \lambda_2', K_{n+1}^m) \leq 1 \tag{5}$$

where K_{n+1}^m refers to the stiffness matrix being reduced *m* times for the critical element of each load step.

A routine with the name "Find μ" is defined in Figure 1. Figure 2 shows the program structure diagram for the imposed loading. The structure state refers to the displacements, velocities and accelerations of the nodes. The parameter *r* is defined as the material equilibrium convergence tolerance value.

Perform a non-linear analysis (Newton-Raphson)	
For all elements	
	Calculate the utilisation value
	Store the maximum utilisation value as μ and the critical element number

Figure 1: Routine "Find μ"

Save structure state			
For all load steps			
	Find μ		
	Repeat if $\lvert\mu\text{-}1\rvert > r$		
		Reduce the stiffness of the critical element	
		Load structure state	
		Find μ	
	Output results		
	Save structure state		

Figure 2: Program structure diagram for the load control

Figure 3 illustrates the searching path of the imposed loading of force control and displacement control separately. *F* and *U* represent the force vector and displacement vector. The blue line is the target curve. The green dotted lines present the load steps. The red dashed lines present the current stiffness, which has been reduced from the previous value based on the stiffness reduction. The black solid arrow lines are the procedure paths for every cycle. The pink solid arrow lines are the output paths for all the cycles in one load step. The solid dots are the equilibrium states while the open dots are the temporary trial states. It is noted that the paths of the black dashed lines result from the internal force change along with the stiffness reduction. The N-R procedure has been performed to update the internal force based on the current displacements and the reduced stiffness. When reaching an equilibrium state, a load increment is applied for the next load step. If the utilization value is still smaller than 1, the next load increment is applied (Step 1→2→3 in Figure 3a). Otherwise, the procedure restarts from the structure state of the previous load step, which means that the displacements are reset to the values of the previous load step. Below, two procedures in one cycle are described:

– Firstly, the secant stiffness of the critical element of the previous cycle is reduced by the defined stiffness reduction factor, which is the same as for SLA. It is noted that the damage procedure is irreversible, which means that all stiffness reductions of the previous cycles are repeated before the current cycle in this load step. Due to these stiffness reduction procedures, the internal forces are updated based on the displacements of the previous load step and the algorithm reaches a temporary equilibrium state, which is calculated by the N-R iterations. One N-R iteration is enough for a geometrically linear analysis. Eq. (6) is adopted to update a temporary equilibrium state for the force control loading while Eq. (7) is employed for the displacement control loading. However, several N-R iterations are needed for a geometrically non-linear analysis.

$$K'\Delta u = F_{ext} - F'_{int} \quad (6)$$

$$K'\Delta u = -F'_{int} \quad (7)$$

where K' is the reduced stiffness, F'_{int} is the updated internal forces due to the reduced stiffness and F_{ext} is the external forces for the force control loading.

– Secondly, the incremental load is applied and a linear analysis is performed for the current load step.

For instance, an equilibrium state starts at Step 8 and ends up at Step 12 (a load step). A new load increment is applied at Step 9. After that, the stiffness is reduced sequentially from Step 10 to Step 12 (cycles). The search path of this load step is Step 8→9→8→8a→10→8→8b→11→8→8c→12.

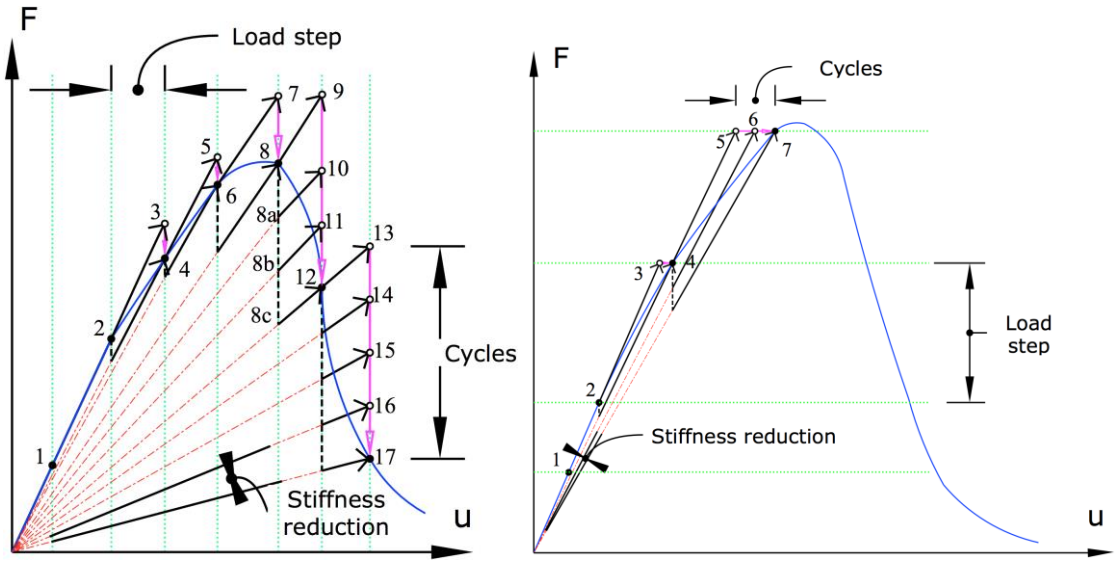

a. Displacement control loading b. Force control loading

Figure 3 Searching path for the load control

2.2 Load scaling control

For the Load scaling control, λ_1 is fixed and λ_2 is incremented or decremented depending on the capacity of the structure, which is based on μ. Two control methods are introduced below in the Load scaling control.

2.2.1 Damage control method

Suppose that after load step *n* somewhere the failure surface is reached.

$$\mu_n = \mu(\lambda_1, \lambda_2, K_n) = 1 \tag{8}$$

For the next cycle

$$\mu_{n+1}^1 = \mu(\lambda_1, \lambda_2^1, K_{n+1}^0) > 1 \tag{9}$$

where λ_2^1 is an increased λ_2 and $K_{n+1}^0 = K_n$. The superscript on λ refer to the cycle number of a load step.

Subsequently, reduce the Young's modulus of the critical element and restart from μ_n

$$\mu_{n+1}^2 = \mu(\lambda_1, \lambda_2^1, K_{n+1}^1) \tag{10}$$

where K_{n+1}^1 is the stiffness matrix with reduced Young's modulus of the critical element.

If μ is still larger than 1, then again restart from μ_n

$$\mu_{n+1}^3 = \mu(\lambda_1, \lambda_2^2, K_{n+1}^1) \tag{11}$$

where λ_2^2 is a reduced λ_2^1 based on a constant reduction q or a function $q(\mu)$ ($\lambda_2^2 = q\lambda_2^1$ or $\lambda_2^2 = q(\mu)\lambda_2^1$). Parameter q is smaller than 1 but larger than λ_2/λ_2^1, e.g. λ_2/λ_2^1 is 0.9 and q is 0.95. Parameter q can be adjusted by a decreasing function $q(\mu)$ where $q(1) = 1$.

If μ is still larger than 1, then repeat restarting from μ_n until

$$\mu_{n+1}^{m+1} = \mu(\lambda_1, \lambda_2^m, K_{n+1}^1) \leq 1 \quad (12)$$

where λ_2^m means that λ_2 is adjusted m times, which is a reduced λ_2^{m-1} based on a constant reduction q or a function $q(\mu)$.

In case of a weakly non-linear situation, the relation between the load factor and utilization function can be linearized. Equations 9 to 12 can be written as

$$\mu_{n+1}^1 = C_0 \quad (13)$$
$$\mu_{n+1}^2 = C_0 + C_1(\Delta E) + C_2\lambda_2^1 \quad (14)$$
$$\mu_{n+1}^3 = C_0 + C_1(\Delta E) + C_2\lambda_2^2 \quad (15)$$

where C_0 represents the value of μ with a new load factor of Load step n+1, ΔE is the stiffness reduction, C_1 represents some non-linear function of ΔE and μ and $C_2\lambda$ represents a linear relation of λ and μ when the stiffness is fixed.

Load factor λ_2^2 can have any values close to but different from λ_2^1. In the practical application, λ_2^2 is defined as λ_2^1 over μ_{n+1}^2. The value of the utilisation function μ should be 1, therefore,

$$1 = \mu_{n+1}^4 = C_0 + C_1(\Delta E) + C_2\lambda_2^3 \quad (16)$$

from which λ_2^3 can be solved.

$$\lambda_2^3 = \lambda_2^1 \frac{(2\mu_{n+1}^2 - 1 - \mu_{n+1}^2\mu_{n+1}^3)}{\mu_{n+1}^2(\mu_{n+1}^3 - \mu_{n+1}^2)} \quad (17)$$

For a strongly non-linear situation, parameter p is defined as an adjustment value which varies depending on μ to render |μ-1| smaller than r. Actually, p is smaller than 1 when μ is larger than 1, and vice versa. Eq. (17) is in fact scaling the load level to the level at which the most loaded element is loaded to just its strength, which is typical for SLA. Figure 4 shows the program structure diagram for Load scaling control.

In this paper, this method is called damage control method because Young's modulus of just the critical element is once reduced and further remains unchanged during load factor adjustment iterations. Like in SLA, only one element is damaged in every load step of the damage control method.

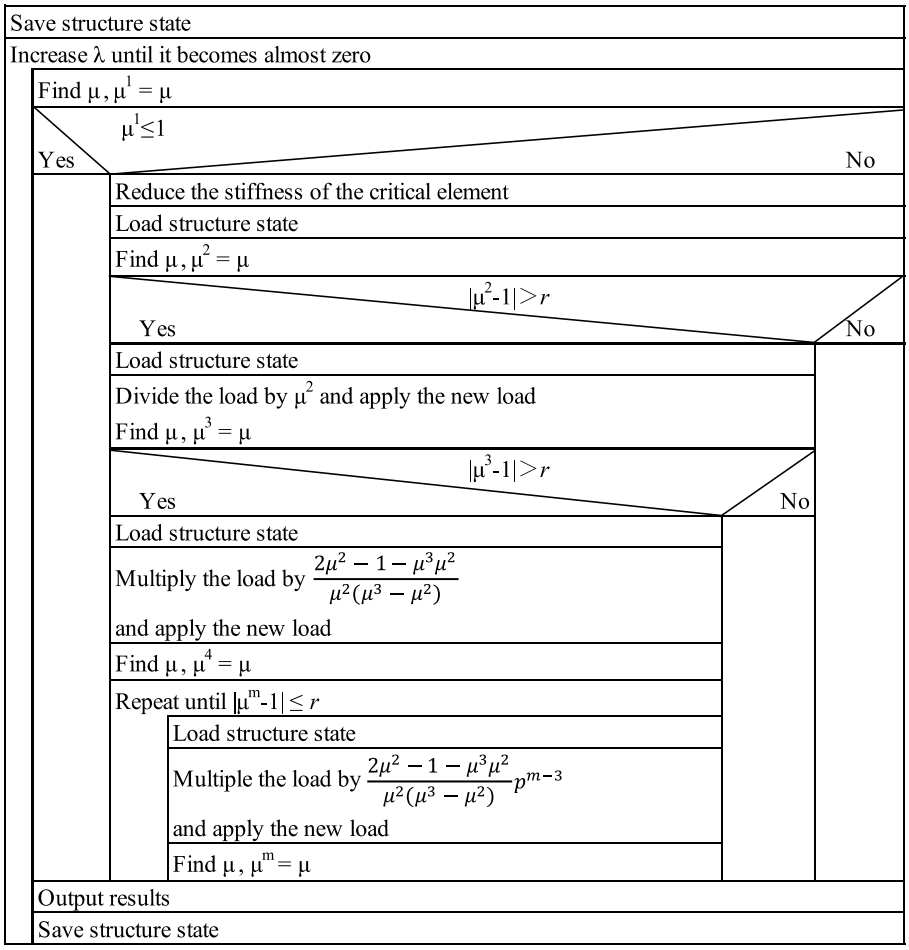

Figure 4: Program structure diagram of the damage control method in Load scaling control

Figure 5 shows the restart procedure of the implicit algorithm. Important is saving and loading of the structure state. Only when |μ-1| is smaller than *r* the structure state will be saved and overwritten. Consequently, the analysis is restarted with the structure state of the last cycle of the previous load step. Without the restart command the algorithm would continue with the structure state of the previous cycle of the current load step, which would be incorrect. This restart procedure ensures that every load step's calculation is based on the correct structure state and stiffness of just the critical element.

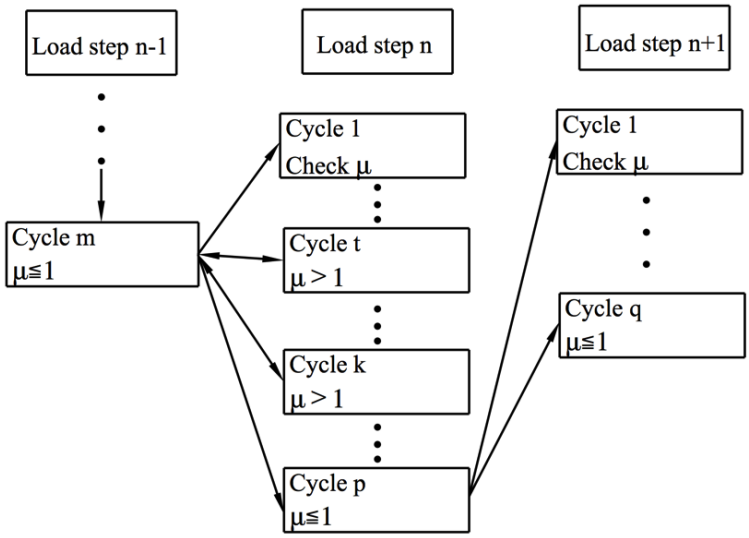

Figure 5. Restart procedure of the algorithm

2.2.2 Load and damage control method

Compared with SLA, the damage control method has more calculating cycles since several extra cycles are necessary (interpolation procedure) for every stiffness reduction to reach an equilibrium state. In order to improve the efficiency for the damage control method, the stiffness matrix is reduced rather than fixed during load factor adjustment iterations. Consequently, the total number of cycles still equals the number of the stiffness reductions. In other words, the total number of cycles is not increased by the load factor scaling procedure.

To this end Eq. 11 and 12 are adjusted. The stiffness matrix is being reduced during the iterations rather than being reduced only once and then fixed.

If μ is larger than 1, then restart from μ_n

$$\mu_{n+1}^{3} = \mu(\lambda_1, \lambda_2^2, K_{n+1}^2) \tag{18}$$

If μ is still larger than 1, then restart from μ_n until

$$\mu_{n+1}^{m+1} = \mu(\lambda_1, \lambda_2^m, K_{n+1}^{\mathrm{m}}) \leq 1 \tag{19}$$

where λ_2^m is a reduced λ_2^{m-1} based on a constant reduction q or a function $q(\mu)$.

The program structure diagram is shown in Figure 6. Figure 7 shows the algorithm path of the Damage control method and the Load and damage control method for applying a force load. *F* and *U* represent the force vector and displacement vector. The blue line is the target curve. The green dotted lines present the load steps. The red dashed lines indicate the reduced stiffness based on the stiffness reduction. The black solid arrow lines are the procedure paths for every cycle. The pink solid arrow lines are the output paths for all the cycles in one load step. The solid dots are the equilibrium states while the open dots are the temporary trial states. It is noted that the paths of the black dashed lines result from the internal force change along with the stiffness reduction. The N-R procedure has been performed to update the internal force based on the current displacements and the reduced stiffness.

Save structure state
Increase λ until it becomes almost zero
Find μ
If μ＞1 — No / Yes
Reduce the stiffness of the critical element
Load structure state
Find μ
Repeat until |μ-1|≤ *r*
Reduce the stiffness of the critical element
Load structure state
Reduce the load
Find μ
Output results
Save structure state

Figure 6. Program structure diagram of Load and damage control method in Load scaling control

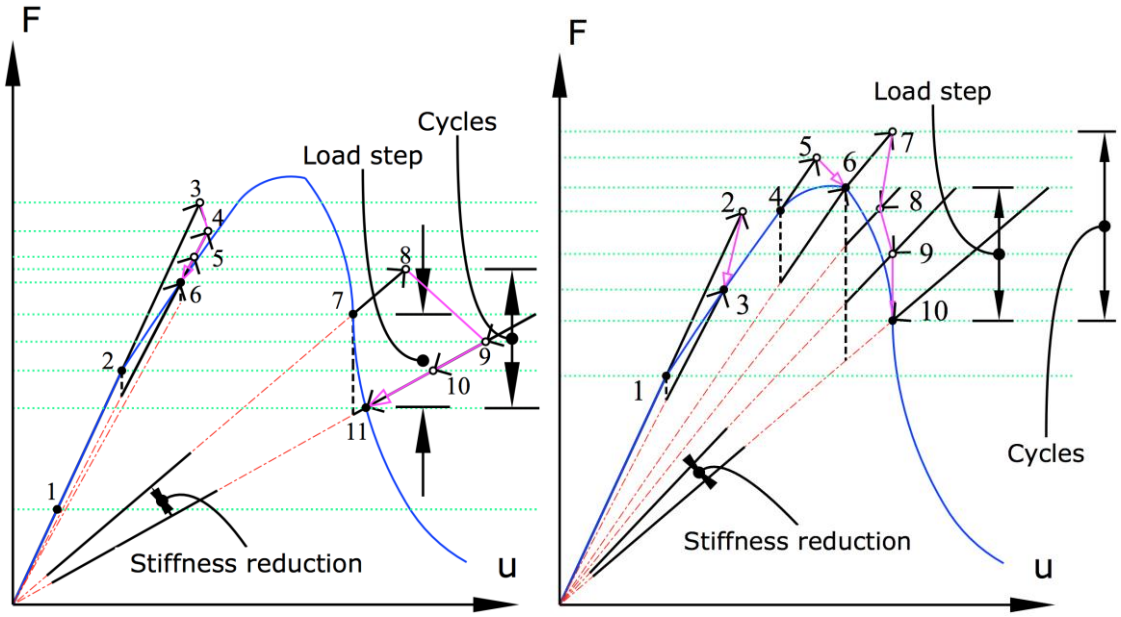

a. Damage control method b. Load and damage control method

Figure 7 Searching path of Load scaling control

To summarize, if the incremental load is prescribed in load steps, it is referred to as the *Load control method*. Here load can be both a prescribed force load increment or a prescribed displacement load increment. If the incremental load is scaled based on the reduced stiffness, it is referred to as the *Load and damage control method*. The latter is especially suitable in case the problem cannot be handled in displacement control for obtaining post-peak behavior. In addition, there is a third algorithm called the *Damage control method*. Here, the stiffness is only reduced once in the first cycle no matter how many cycles the load step has. Since the stiffness remains unchanged after the first cycle, the scaling procedure follows a linear interpolation procedure to search for the suitable load factors. It is quite similar to SLA in that the algorithm reaches an equilibrium state for every damage step and the load factors are governed by the utilization value. But the difference is that in ISLA every equilibrium state

search starts from the equilibrium state of the previous "load step", which indeed is the previous damage step, instead of restarting from the origin in the total scheme of SLA. However, in the *Load and damage control method* the stiffness is continued to be reduced every cycle. So, the number of stiffness reductions is the same as that of the cycles in the load step.

3. Highly prestressed beam test

In [29], the principle, algorithms and search paths of incremental sequentially linear analysis has been demonstrated for the case of proportional loading of a simply supported notched beam. In that publication, the effectiveness of the scheme with cycles has been illustrated in detail for a number of typical prescribed load steps. Plots of the number of cycles per load step, element criticality and stress-strain jumps illustrate the searching path.

The example in the present section focuses on the robustness of this method for non-proportional loading. To this end, the beam mentioned before [29] has been re-used without a notch and subjected to the combination of a horizontal prestress *P* at both ends of the beam and a vertical load *L* at the top, as illustrated in Figure 8. This beam is adapted from Hordijk's experiment in 1981 [30]. It has also been used in [16] [17]. *P* is applied as a stress of 1, 5 or 10 MPa over the total area of the beam ends instead of 1 MPa as used before [16] [17]. *L* is applied as two point loads up to and beyond the peak, which increase to failure and reduce afterwards. No reinforcement is applied.

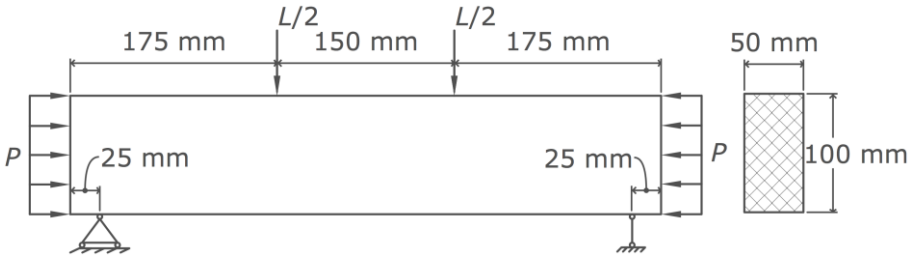

Figure 8. Test model dimension and load combination

3.1 Material properties and modified material model

This case considers softening for tension. The concrete properties are E = 32000 MPa, Poisson's ratio = 0.2, tensile strength f_t = 3 MPa, fracture energy G_f = 0.06 N/mm. The compressive behaviour is elastic. Eq. 18 is used to determine the ultimate strain to consider mesh size dependency (Figure 9).

$$G_{\mathrm{f}} = \frac{f_t \varepsilon_u h}{2} \tag{18}$$

where h is the element size and ε_u is the strain at which the concrete is completely fractured. This paper does not consider mesh directional dependency. Mesh directional bias has been studied in [31][32][33]. Possible solutions include non-local damage models [34][35], the strong discontinuity approaches [36][37] and the extended finite element method [38][39].

Figure 10 shows the analysis cycles when Young's modulus is sequentially reduced to 50% of the previous value (The virtual strength is 4.22 MPa). In this paper a reduction factor of 90% has been used. This has not been displayed here because it would produce an unclear picture.

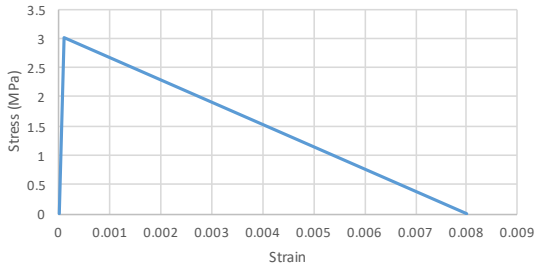

Figure 9. Material properties of concrete (tension softening)

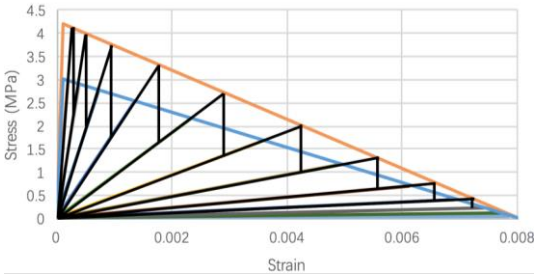

Figure 10. Stiffness reduction procedure: sequentially reduced stiffness to 50% of the previous value

3.2 FEM model in ABAQUS and ANSYS

The analyses have been performed by 1) Standard N-R with force control in ABAQUS, 2) Standard N-R with arc length control in ABAQUS, 3) SLA in ANSYS [8] and 4) the proposed method in ANSYS. The same material properties, element sizes (5 mm) and structural model have been used in all analyses (Figure 8). In ANSYS the rotating smeared crack model is used. In ABAQUS the concrete damaged plasticity model is used to simulate concrete behaviour. The parameters inputted for this model are: dilation angle is 30° , eccentricity is 0.1, f_{b0}/f_{c0} = 1.16, K = 0.667, and viscosity parameter is 0 [40].

The plane element used in ABAQUS is CPS8R, which is an 8-node biquadratic plane stress quadrilateral with reduced integration. The plane element used in ANSYS is PLANE183. It is a higher order 2-D, 8-node element. The integration point scheme for both element types is 2x2 Gauss.

Figure 11 shows the colour range of the maximum principal strain contours.

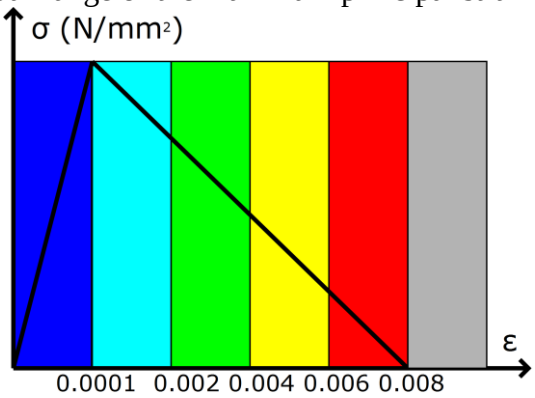

Figure 11. Contour color range

3.2 Comparison for 1 MPa prestress

The original 1 MPa prestress [16] [17] is applied for comparison. Figure 12 indicates that the proposed method and SLA deliver almost the same force-displacement diagram. Moreover, one crack is localized and propagates to the top of the beam for both methods shown in Figure 13 and Figure 14. Actually, the plateau of the curve can continue to extend to more than 10 mm. These two methods produce almost identical results for the 1 MPa prestress test. Both of them have no divergence issues.

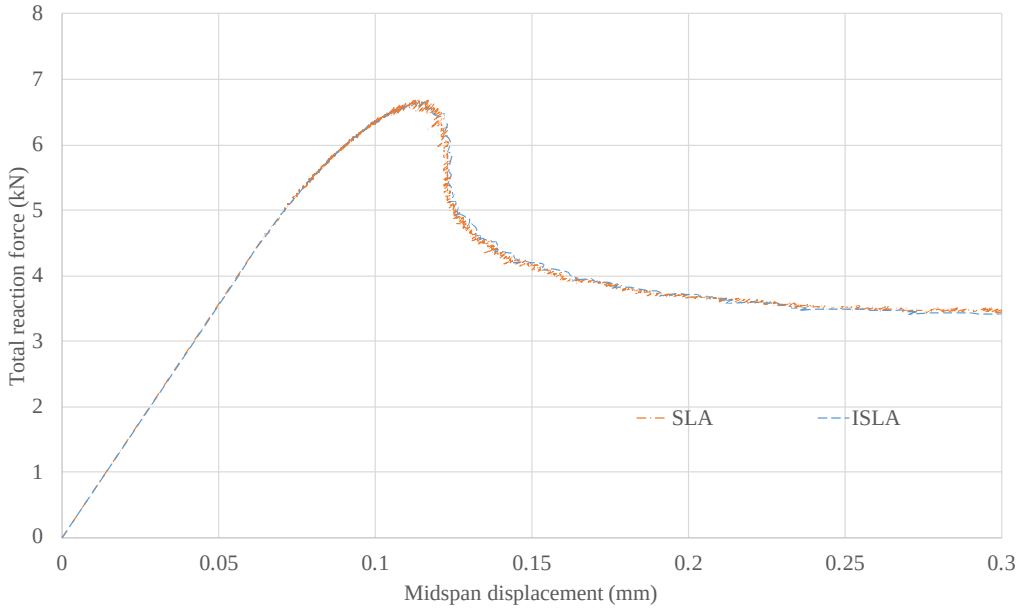

Figure 12 Reaction force-displacement diagrams for the 1 MPa prestress test

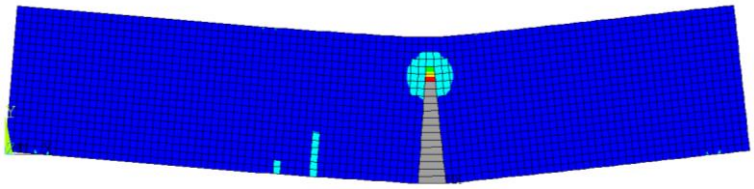

Figure 13 Maximum principal strain contour when the midspan displacement is 0.3 mm by the proposed method for the 1 MPa prestress test

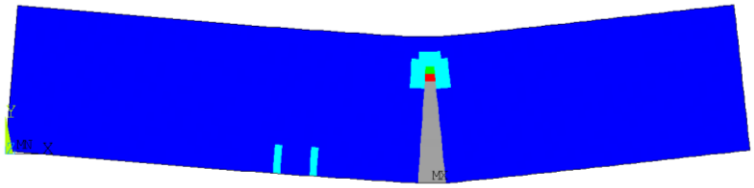

Figure 14 Maximum principal strain contour when the midspan displacement is 0.3 mm by SLA for the 1 MPa prestress test

3.3 Comparison for 5 MPa prestress

Figure 15 shows the force displacement diagrams for 5 MPa prestress of ISLA, N-R and SLA with marked deviation points of SLA and N-R. The SLA analysis stops at a displacement of 1.8 mm while ISLA can continue up to 2.2 mm and further. The cracks have already propagated to the top of the beam at the displacement of 2.2 mm in ISLA. Hence the ISLA results beyond this point are not shown. The diagram of SLA is quite similar, but the N-R method fails earlier. The reason for the SLA algorithm to stop at 1.8 mm displacement is explained here. Initially, the constant-load factor v can be adjusted to almost equal to the varying-load factor λ as shown in Figure 16. However, after 1.8 mm displacement the constant-load factor v cannot be adjusted to equal the live load factor λ as shown in Figure 17. It appears that the algorithm of non-proportional loading in SLA [16] as well as [17] is only suitable for weakly non-linear situations.

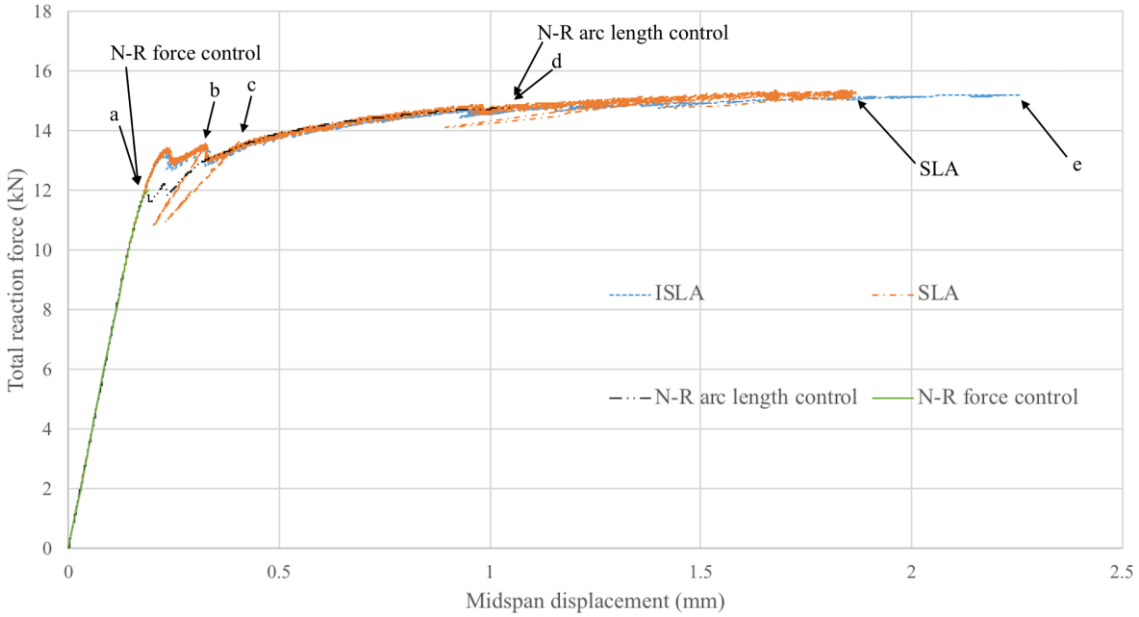

Figure 15. Reaction force-displacement diagrams for the 5 MPa prestress test

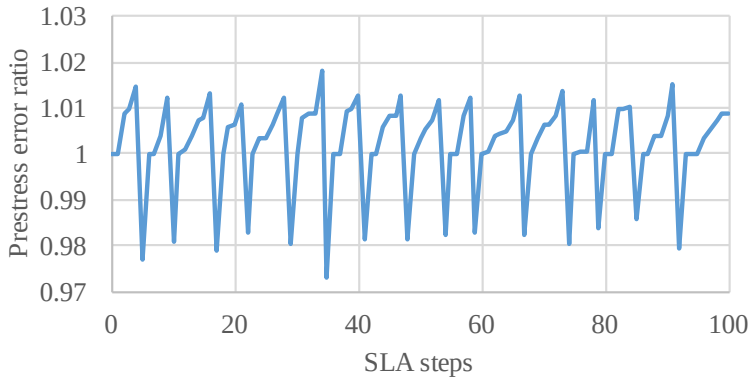

Figure 16. Prestress adjusting ratio ν/λ for the SLA analysis: The first 100 cycles are shown as an example of convergence to the correct value.

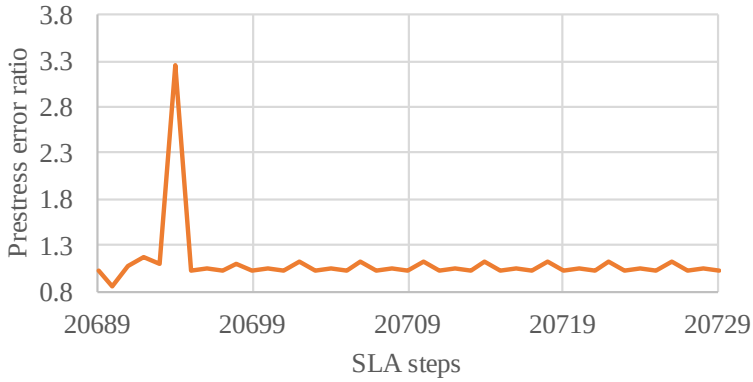

Figure 17. Prestress adjusting ratio ν/λ for the SLA analysis: 41 cycles are shown. All shown cycles fail to convergence. (The peak has no particular meaning.)

Figure 18 shows the crack propagation calculated by the proposed method, at 5 stages, which are marked in Figure 15. Initially, symmetrical ductile cracks occur at the bottom of the beam and the maximum principal strain of two symmetrical critical elements go into the green zone in Figure 18a. At this moment, the displacement-reaction force diagram meets the end point

of the initial slope. Afterwards, the right critical crack propagates much faster than the left one until the displacement-reaction force diagram reaches the first peak shown in Figure 18b. After that, the displacement-reaction force diagram drops a little and then rises to a second peak when the left critical crack catches up with the right one in Figure 18c. Then the development of the left critical crack even surpasses the right one in Figure 18d. Finally, the main cracks bifurcate, with branch cracks forming and extending to the top of the beam in Figure 18e. There is no further damage due to the elastic compressive capacity. Similar crack propagation is obtained by SLA, for which the final crack pattern is shown in Figure 19. The spacing of cracks is governed by the positions of the critical elements which have the largest ratio of the maximum principal stress versus strength in a cycle. Initially multiple elements can be critical and cracks start in a distributed manner, but eventually only two dominant cracks survive while other elements are unloaded. It is an advantage of SLA and ISLA to handle bifurcations properly. For a four-point loaded beam, two dominant cracks are underneath the loading positions.

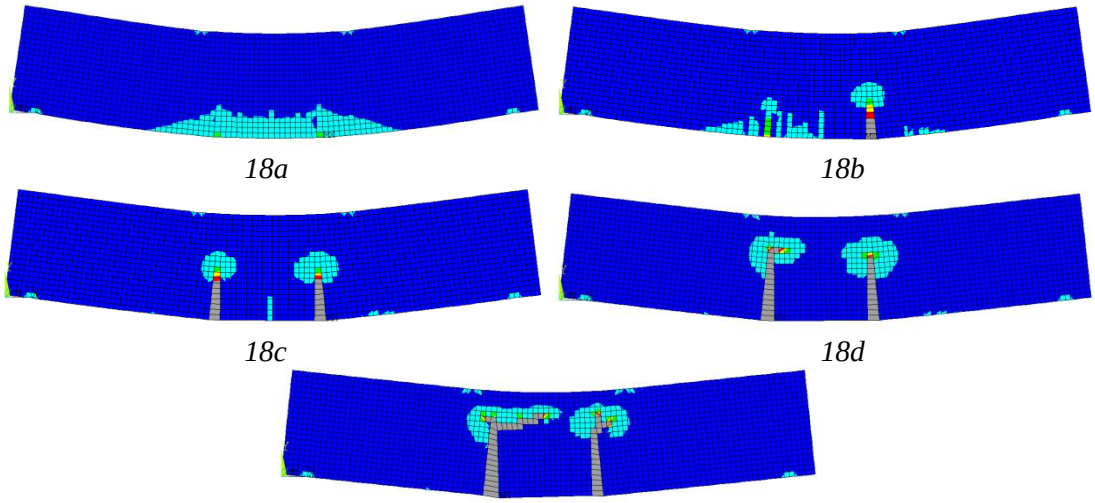

18a *18b*

18c *18d*

18e

Figure 18. Maximum principal strain contours of crack propagation by the proposed method for the 5 MPa prestress test

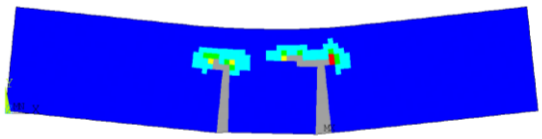

Figure 19. Maximum principal strain contour of final crack pattern by SLA for the 5 MPa prestress test

Figure 15 shows that the reaction force-displacement diagrams of the ABAQUS N-R analysis can only reach the end point of the initial slope although the structure almost has hardening behaviour. The value of initial slope is the same for SLA and the proposed method. The crack pattern is also similar but has fewer cracks (Figure 20).

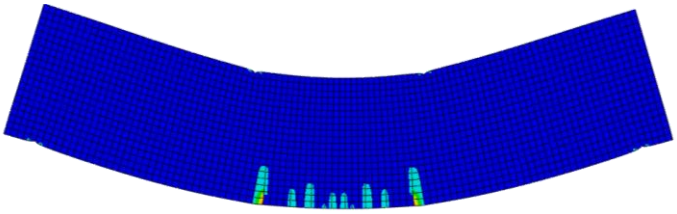

Figure 20. Maximum principal strain contour of final crack pattern by N-R force control analysis for the 5 MPa prestress test

Only extremely small load steps (1e-7 at the end) with arc-length control can find the hardening part of the reaction force-displacement diagram shown in Figure 15. The first peak is lower than SLA and the proposed method, nevertheless they align well after the second peak. After that they both have a similar hardening slope. As shown in Figure 21, the ultimate crack pattern is similar to that of the proposed method and SLA while it has less cracks at the end point of the initial slope and the first peak, which results in lower capacity than SLA and the new method.

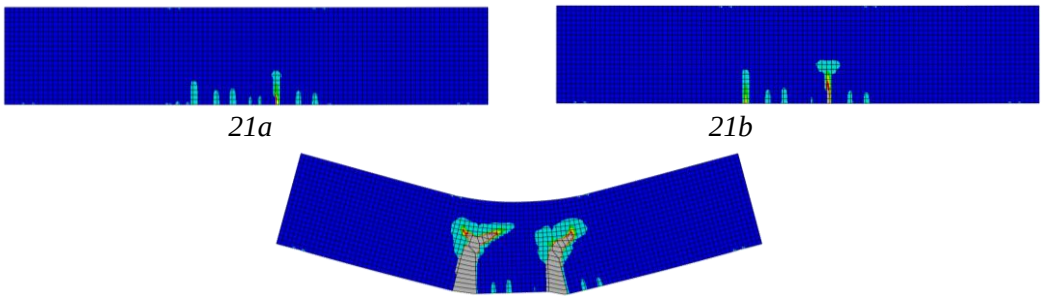

Figure 21. Maximum principal strain contours of the crack propagation of the N-R arc length control analysis for the 5 MPa prestress

3.4 Comparison for 10 MPa prestress

Figure 22 shows the reaction force-displacement diagrams for 10 MPa prestress of SLA and the proposed method with marked deviation points of SLA and N-R. They overlap in the beginning of the curves. SLA fails to continue earlier than the 5 MPa prestress test and does not reach the final hardening slope. N-R arc length even diverges before N-R force control.

Figure 23and Figure 24 show the crack patterns for the proposed method and for SLA, which are marked in Figure 22. In SLA, the numerical procedure stops at the stage of two major symmetrical cracks. The proposed method continues and also shows the formation of branch cracks. The main difference with the crack development in the 5 MPa prestress test is that two dominant cracks develop simultaneously. It is because the higher prestress has a higher effect in preventing cracks to propagate to the top of the beam.

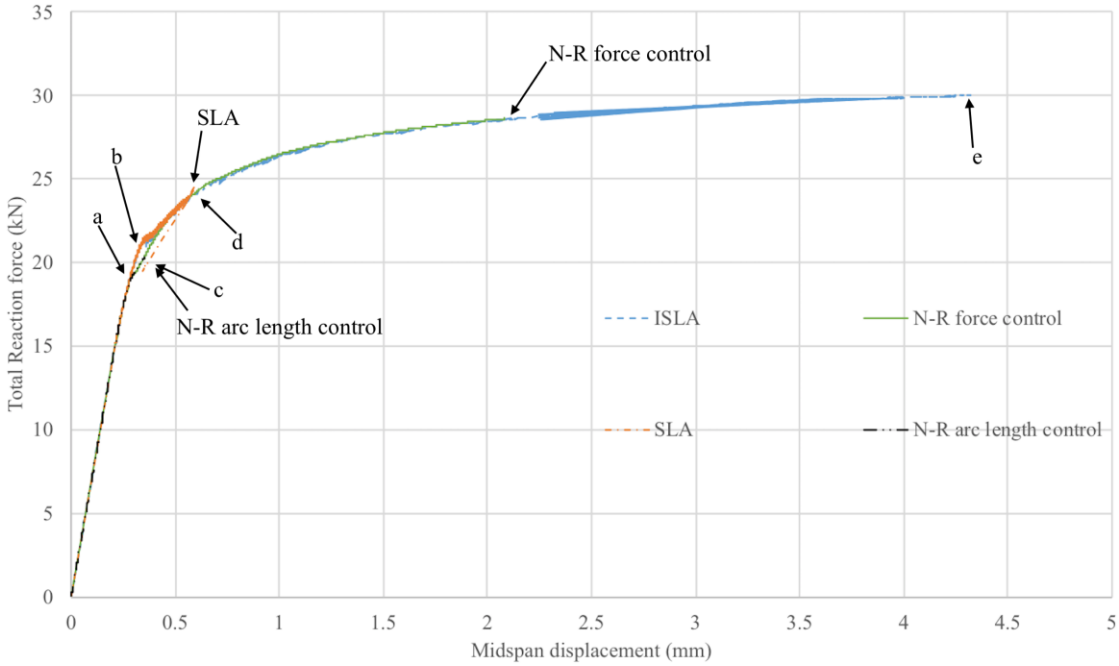

Figure 22. Reaction force-displacement diagram for the 10 MPa prestress

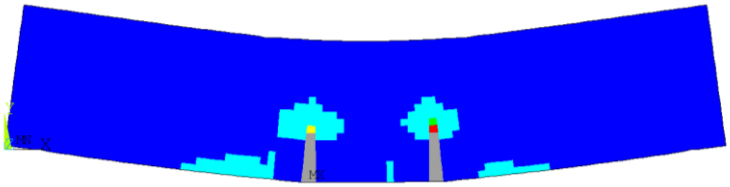

Figure 23. Maximum principal strain contour of the final crack pattern of SLA for the 10 MPa prestress

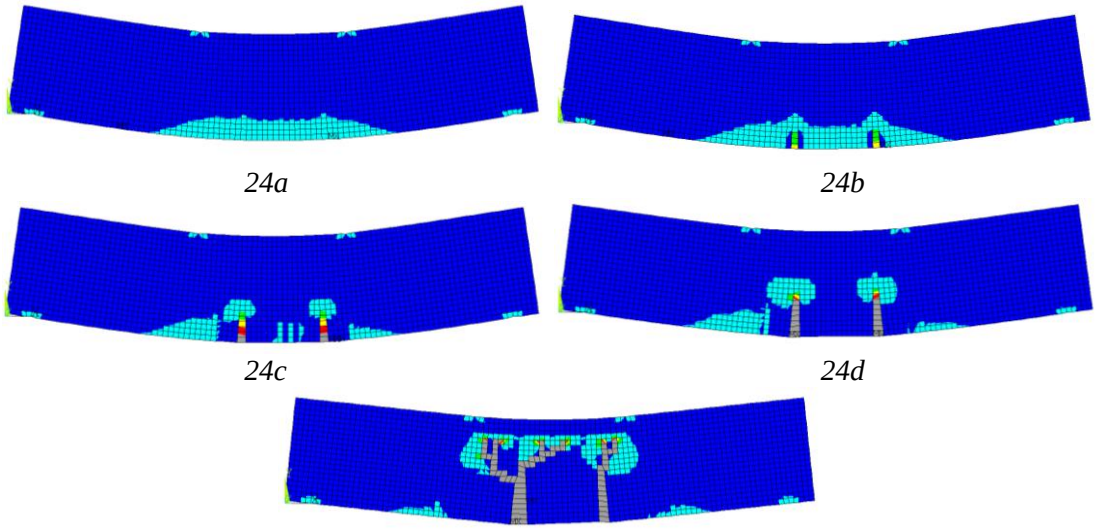

24a *24b*

24c *24d*

24e

Figure 24. Maximum principal strain contours of the crack propagation of the proposed method for the 10 MPa prestress

The reaction force-displacement diagram of the Newton-Raphson method with force control has a good agreement with SLA and the proposed method from the initial slope to the final hardening slope (Figure 22). The hardening behaviour can be obtained without arc length

method. Figure 25 also shows symmetrical crack development in N-R force control even until the branch crack moment whereas the proposed method has random branch cracks.

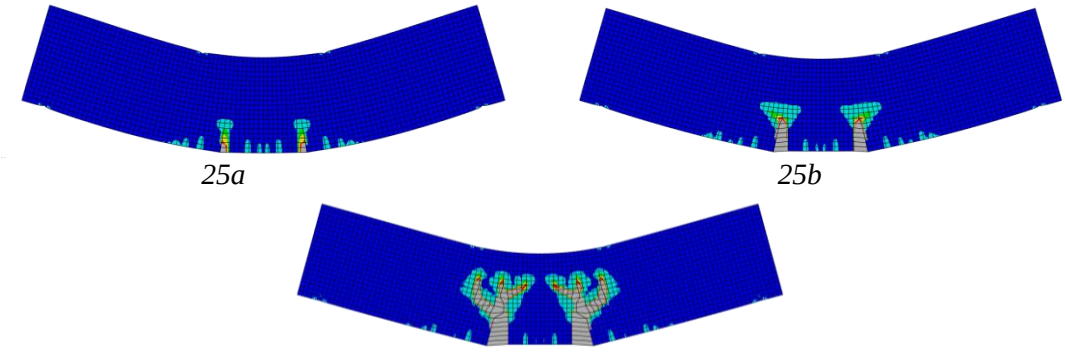

25a *25b*

25c

Figure 25. Maximum principal strain contours of the crack propagation by N-R force control for the 10 MPa prestress

Figure 26 shows numbers of cycles of every load step in ISLA. For the 5 MPa prestress test, the total number of cycles of ISLA is 13047 while that of SLA before divergence is 20688. The total number of increments for the N-R arc length control is 258958. The very small arc length has to be employed in order to reach convergence, while each increment has several iterations. The maximum number of cycles of a load step in ISLA is 23. For the 10 MPa prestress test, the total number of cycles of ISLA is 18936 while that of SLA before divergence is 7519. The total number of cycles of SLA for 10 MPa prestress test is smaller than that of ISLA is because SLA diverges very early. The maximum number of cycles of a load step in ISLA is 21. From these numbers it is clear that ISLA used the lowest number of computation steps. Nevertheless, it is recommended to further improve the efficiency of ISLA by reducing the number of cycles.

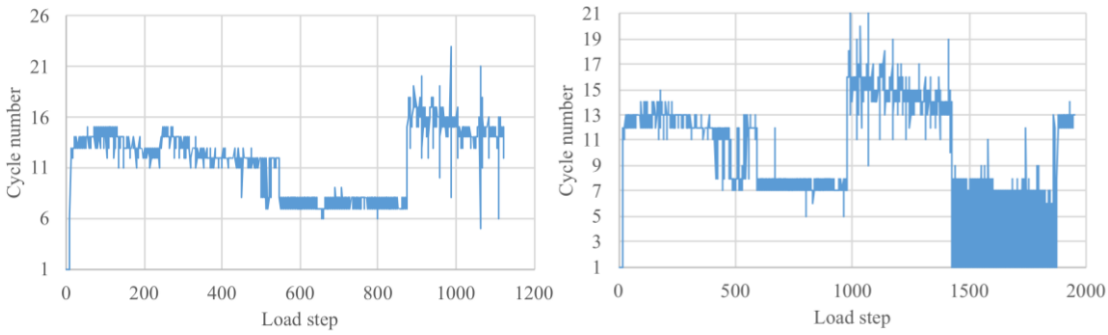

26a 5 MPa prestress test *26b* 10 MPa prestress test

Figure 26. Numbers of cycles of every load step in ISLA

The strength limit of the beams can be calculated by hand from equilibrium. This is due to the linear elastic compression zone. The limit strength of the total reaction force is

$$F = P\frac{h-d}{a},$$

where P is the prestressing force (uniformly applied), h is the beam depth, d is the element size (4-node element with 1 integration point) and a is the horizontal distance between a load and a support reaction. The limit strength with 5 MPa prestress is 15.8 kN; The limit strength with 10 MPa prestress is 31.6 kN, which are in a good agreement with the computational results.

4. Physical and geometrical non-linear analysis test

ISLA is an incremental procedure. Therefore, geometrically non-linear effects can be naturally included in ISLA. When geometrically non-linear effects are considered, the B matrix and geometrical non-linear matrix (which is related to internal forces) are implemented and updated by the Lagrange method. Only the material matrix is updated by ISLA.

TUD-COMP-0b is a quasi-static one-way out-of-plane tests administered by TU-Delft [41]. This specimen was a single-wythe wall constructed of calcium silicate units 102 mm thick. It was 1.4 metres long and 2.75 metres high. The wall is subjected to a constant overburden load of 0.2 MPa and is subsequently subjected to a uniform face pressure load via airbags. The wall is fully clamped at its base. For the top boundary, the horizontal in-plane and out-of-plane translations are fixed, as well as all rotations, but the top boundary is free to displace vertically. The two side supports are free. The FEM model is shown in Figure 27.

The one-way bending gives a crack at top and bottom and in the middle of the wall This leads to a three-hinged mechanism where the geometrically non-linear effect governs post-peak softening behaviour.

4.1 Modelling approach

Table 1 depicts model information. The analyses have been performed by 1) Geometrically linear and physically non-linear arc length control analysis in ABAQUS, 2) Geometrically and physically non-linear arc length control analysis in ABAQUS, 3) Geometrically linear and physically non-linear SLA in ANSYS and 4) Geometrically and physically non-linear ISLA in ANSYS.

The same material properties, element sizes (0.1m x 0.1m) and structural model have been used in all analyses. To simulate the loading frame, two 2.4 m beams are tied to the top and bottom of the wall respectively with 6 DOFs. At phase one, 30 kN line load corresponding to 0.2 MPa overburden is applied at the top beam in Y direction. Then at phase two, lateral pressure is applied at the whole wall.

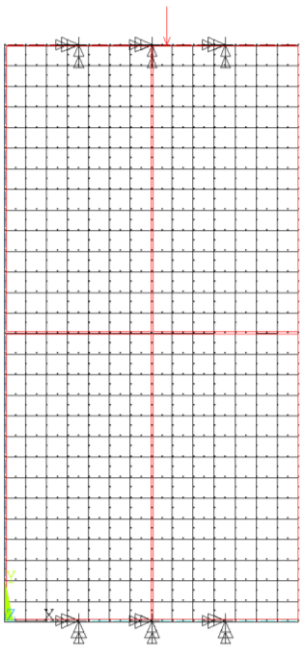

Figure 27 FEM model

Table 1. Model loading, geometry, material properties and boundary conditions

Loading			
Dead load	Self-weight		
Overburden	0.2	MPa	
Estimated lateral pressure	4000	kPa	
Geometry	Value		Description
wbr =	0.214	m	Horizontal dimension of bricks
hbr =	0.071	m	Vertical dimension of bricks
tbr =	0.102	m	Brick thickness
L =	1.4	m	Length of wall
H =	2.75	m	Height of wall/building
Steel material properties	Value		Description
E =	2.1×10^{11}	N/m^2	Steel Young's modulus
ν =	0.3		Poisson's ratio
Masonry material properties	Value		Description
ρ =	1800	kg/m^3	Mass density
E =	3.5×10^{9}	N/m^2	Masonry Young's modulus
ν =	0.21		Poisson's ratio
f_t =	1.5×10^{5}	N/m^2	Masonry tensile strength
G_f =	15	N/m	Fracture energy for tensile failure
Boundary conditions	Description		
Base	Clamped		
Top	· In- and out-of-plane translation fixed. Free to displace vertically		

	· Rotation fixed in all directions

4.2 Test results

Figure 28 shows the midspan displacement versus base shear force diagrams for 1) Geometrically and physically non-linear ISLA, 2) Geometrically linear and physically non-linear SLA, 3) Geometrically linear and physically non-linear Newton–Raphson method and 4) Geometrically and physically non-linear Newton–Raphson method. The deviation points of N-R and SLA are marked in the figure. It can be observed that the peak capacities meet well for these four analyses. However, the geometrically non-linear effect governs post-peak softening behaviour. Both geometrical linear analyses from SLA and Newton–Raphson method have a hardening behaviour after the peak. For all three methods, the total load meets the peak 10 kN at 2.6 mm and the peak plateau keeps stable until the displacement is 5.6 mm. Then the total load drops below 8 kN when the midspan displacement increases to 9 mm. Then, the total load becomes almost zero when the ultimate displacement is approximately 100 mm (98 mm).

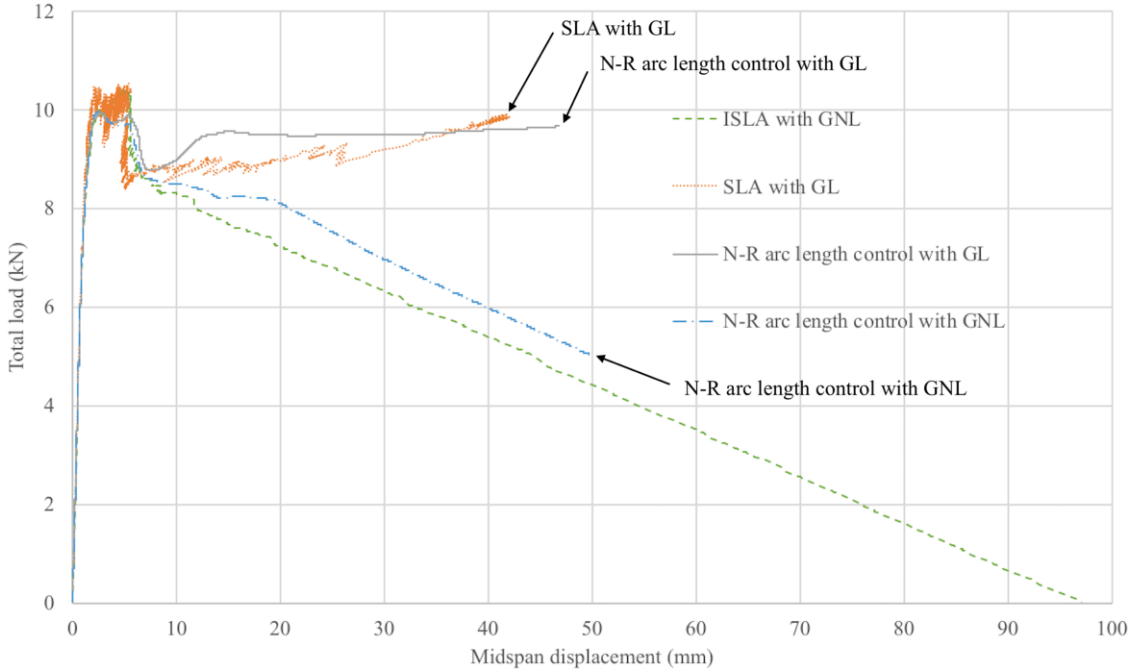

Figure 28. Midspan displacement-force curves for comparison of geometrical linear and non-linear effects

5. Discussion

The new algorithm extends sequentially linear analysis to classical non-linear implicit analysis with Newton-Raphson iterations. The name we propose for this solution method is incremental sequentially linear analysis (ISLA): the words “sequentially” and “linear” refer to the established sequentially linear analysis from which the method is derived; the word incremental refers to the incremental procedure.

Indeed, an implicit scheme is chosen in this paper. However, an explicit scheme can also be used in the algorithm. The main difference would be that the algorithm does not restart from the previous equilibrium state to update incremental displacements.

In the load control method, every load step can contain one increase or decrease of the load and several reductions of Young's modulus of various elements. In the damage control method, every load step can contain one reduction of Young's modulus and several changes of the load. In the load and damage control method, every load step can contain several changes of the load and several reductions of Young's modulus of various elements. Table 2 shows the differences of these methods.

Table 2. Changes in load and Young's modulus within one load step

ISLA	Load	Young's modulus
Load control method	Once increased or decreased (prescribed loading)	Several reductions for one or more critical elements
Damage control method	Once increased and then several changes (scaled loading)	One reduction for one critical element
Load and damage control method	Once increased and then several changes (scaled loading)	Several reductions for one or more critical elements

For the imposed displacement loads, it is recommended to use the load control method. For the force loads, this method can be used too but the post peak response cannot be obtained. The damage control method can be used to determine the post peak behaviour and snap back behaviour of structures. The load and damage control method is much faster than the damage cycle method. It is also robust and it provides the same results. Based on efficiency, the load control method and the load and damage control method are suggested for large structures.

6. Comparison of SLA and ISLA

Sequentially linear analysis (SLA) and incremental sequentially linear analysis (ISLA) have several features in common. Young's modulus of the material around a critical integration point is reduced. The critical integration point is defined as the point with the largest utilisation factor. The load is adjusted to make the largest utilisation factor equal to one. In other words, all integration points pass the utilisation factor check.

On the other hand, there are also differences between SLA and ISLA, which are shown in Table 3.

<table>
<tr><td colspan="2">SLA</td><td rowspan="2">ISLA</td></tr>
<tr><td>proportional loading</td><td>non-proportional loading [17]</td></tr>
<tr><td>unit load is mapped back linearly</td><td>load factor is solved in 3 cycles</td><td>load factor is incremented or decremented</td></tr>
<tr><td colspan="2">displacements are not saved</td><td>displacements are saved</td></tr>
<tr><td>one linear elastic analysis in each load step</td><td>several linear elastic analyses in each load step</td><td>several nonlinear analyses in each load step</td></tr>
</table>

Table 3. Differences between SLA and ISLA

7. Conclusions

This paper proposes the incremental sequentially linear analysis (ISLA). This method is incremental; each increment starts and ends with an equilibrium state. The solution search path follows damage cycles sequentially with secant stiffness.

- The proposed method has a similar high robustness as SLA. It is also user friendly without mapping back procedure in SLA. In addition, it produces smooth curves like [9] instead of the usual jumpy curves of SLA.
- The searching path of ISLA is based on physical parameters (damage history and displacement history) instead of numerical parameters in other methods. The equilibrium state is updated based on stiffness reductions of critical elements and load increments. The damage is also introduced to the structure correctly at the corresponding displacements.
- The proposed method can be easily implemented in commercial software. The results are reproducible. The algorithm does not switch between methods and therefore does not depend on the value of switch parameters.
- Non-proportional loading can be analysed without modifications. There is no restriction on the load definition; load cases can be applied and removed simultaneously or separately.
- The method is an incremental procedure and can be naturally extended to geometrically non-linear analysis and transient analysis.
- Non-proportional SLA as proposed in reference [17] does not converge for high prestressing values on the specimens analysed in this paper. Currently, it is not clear whether regular SLA can be expected to solve this. ISLA on the other hand does converge.
- Large prestressing values prevent softening of the force-displacement relation while the stress-strain relation does soften.
- The proposed method cracks grow one after the other intermittently, whereas the cracks grow simultaneously in the non-linear Newton-Raphson method with arc length control.
- The bending cracks in the specimens branch into multiple cracks. For accurate computation of the crack branches the Newton – Raphson method with arc length control needs a very small step size and a lot of computation time. The proposed method also need much computation time but is still faster than the Newton – Raphson method with arc length control.
- The point at which the bending cracks branch into multiple cracks is higher for 5 MPa prestressing than for 10 MPa prestressing. For even higher prestressing values the crack branching starts directly at crack initiation. On the other hand, for low prestressing values like in reference [17] this point is higher than the beam height, which results in no branch cracks and a softening force-displacement curve.

REFERENCES

[1] R.D. Borst, M.A. Crisfield, J.J.C. Remmers, and C. V. Verhoosel. *Nonlinear finite element analysis of solids and structures*. John Wiley & Sons, 2012.
[2] G.A.Wempner, Discrete approximations related to nonlinear theories of solids, *International Journal of Solids and Structures* 7, 1581 (1971).

[3] E. Riks, An incremental approach to the solution of snapping and buckling problems, *International Journal of Solids and Structures* 15, 529 (1979).
[4] E.Ramm, Strategies for tracing the nonlinear response near limit points, *Nonlinear finite element analysis in structural mechanics* (Springer, 1981) pp. 63–89.
[5] T. Pohl, E. Ramm and M. Bischoff, Adaptive path following schemes for problems with softening, *Finite Elements in Analysis and Design* 86, 12 (2014).
[6] C. V. Verhoosel, J. J. Remmers and M. A. Gutiérrez, A dissipation-based arc-length method for robust simulation of brittle and ductile failure, *International Journal for Numerical Methods in Engineering* 77, 1290 (2009).
[7] J. Oliver, A. Huespe, S. Blanco, and D. Linero, Stability and robustness issues in numerical modeling of material failure with the strong discontinuity approach, *Computer Methods in Applied Mechanics and Engineering* 195, 7093 (2006).
[8] J. Oliver, A. Huespe, and J. Cante, An implicit/explicit integration scheme to in- crease computability of non-linear material and contact/friction problems, *Computer Methods in Applied Mechanics and Engineering* 197, 1865 (2008).
[9] W.Alnaas, *Nonlinear finite element analysis of quasi-brittle materials*, Ph.D. thesis, Cardiff University (2016).
[10] P. Ladevèze. Nonlinear computational structural mechanics: new approaches and non-incremental methods of calculation. *Springer Science & Business Media*, 2012.
[11] Y. F. Gao and A. F. Bower, A simple technique for avoiding convergence problems in finite element simulations of crack nucleation and growth on cohesive interfaces, *Modelling and Simulation in Materials Science and Engineering* 12(3), 453 (2004).
[12] J.G. Rots. Sequentially linear continuum model for concrete fracture. *Fracture Mechanics of Concrete Structures*, 13, 2001.
[13] J.G. Rots, B. Belletti, and S. Invernizzi. Robust modeling of rc structures with an "event-by-event" strategy. *Engineering Fracture Mechanics*, 75(3):590–614, 2008.
[14] J.G. Rots and S. Invernizzi. Regularized sequentially linear saw- tooth softening model. *International Journal for Numerical and Analytical Methods in Geomechanics*, 28(7-8):821–856, 2004.
[15] A.T. Slobbe, M.A.N. Hendriks, and J.G. Rots. Sequentially linear analysis of shear critical reinforced concrete beams without shear reinforcement. *Finite Elements in Analysis and Design*, 50:108–124, 2012
[16] M.J. DeJong, M.A.N. Hendriks, J.G. Rots. Sequentially linear analysis of fracture under non-proportional loading. *Engineering Fracture Mechanics* 75 (2008) 5042–5056
[17] Chenjie Yu, P.C.J. Hoogenboom, J.G. Rots, Algorithm for non-proportional loading in sequentially linear analysis. *9th International Conference on Fracture Mechanics of Concrete and Concrete Structures*, UC Berkeley, 2016
[18] A. Graaf, *Sequentially linear analysis for simulating brittle failure*, PhD Dissertation, Delft University of Technology, ISBN 978-94-6186-799-5
[19] G. Giardina, A. Graaf, M.A.N. Hendriks, J. G. Rots, and A. Marini. Numerical analysis of a masonry façade subject to tunnelling-induced settlements. *Engineering structures*, 54:234–247, 2013.
[20] JGM Van Mier, A Vervuurt, and E Schlangen. Boundary and size effects in uniaxial tensile tests: a numerical and experimental study. *Fracture and Damage in Quasibrittle Structures*, pages 289–302, 1994.
[21] HEJG Schlangen. Experimental and numerical analysis of fracture processes in concrete. *HERON*, 38 (2), 1993.
[22] John E Bolander and N Sukumar. Irregular lattice model for quasistatic crack propagation. *Physical Review B*, 71(9):094106, 2005.

[23] W.F. Alnaas, A.D. Jefferson. A smooth unloading--reloading approach for the nonlinear finite element analysis of quasi-brittle materials. *Engineering Fracture Mechanics* 152 (2016) 105-125
[24] F. Cazesa, G. Meschkeb and Meng-Meng Zhou. Strong discontinuity approaches: An algorithm for robust performance and comparative assessment of accuracy. *International Journal of Solids and Structures* 96 (2016) 355–379
[25] R. Graça-e-Costa, J. Alfaiate, D. Dias-da-Costa, L. J. Sluys, A non-iterative approach for the modelling of quasi-brittle materials. *International Journal of Fracture* (2012) 178:281–298
[26] A.S. Al-Sabah and D.F. Laefer. Use of negative stiffness in failure analysis of concrete beams. *Engineering Structures*, 126:187–199, 2016.
[27] J. Eliáš, P. Frantík, M. Vořechovský, Improved sequentially linear solution procedure. *Engineering Fracture Mechanics* 77 (2010) 2263–2276
[28] J. Eliáš, Generalization of load–unload and force-release sequentially linear methods. *International Journal of Damage Mechanics* 2015, Vol. 24(2) 279–293
[29] Chenjie Yu, P.C.J. Hoogenboom, J.G. Rots, Incremental Sequentially Linear Analysis of a Notched Beam. *Euro-C 2018*, Bad Hofgastein, Austria.
[30] D.A. Hordijk, *Local approach to fatigue of concrete*, PhD Dissertation, Delft University of Technology, ISBN 90-9004519-8
[31] M. Cervera, M. Chiumenti, Mesh objective tensile cracking via a local continuum damage model and a crack tracking technique. *Computer Methods in Applied Mechanics and Engineering*, 196:304–320, 2006. 12, 13, 17, 18, 20, 40
[32] M. Jirasek, P. Grassl, Evaluation of directional mesh bias in concrete fracture simulations using continuum damage models. *Engineering Fracture Mechanics*, 75:1921– 1943, 2008. 14, 40
[33] A.T. Slobbe, *Propagation and band width of smeared cracks*, PhD Dissertation, Delft University of Technology (2015)
[34] Z.P. Bazant, , G.D. Luzio, Nonlocal microplane model with strain-softening yield limits. *International Journal of Solids and Structures*, 41:7209–7240, 2004. 40
[35] Z.P. Bazant, F.B. Lin, Nonlocal smeared cracking model for concrete fracture. *Journal of Structural Engineering*, 114:2493–2510, 1988. 40
[36] T. Belytschko, J. Fish, and B. E. Engelmann, A finite element with embedded localization zones, *Computer methods in applied mechanics and engineering* 70, 59 (1988).
[37] J. C. Simo, J. Oliver, and F. Armero, An analysis of strong discontinuities induced by strain-softening in rate-independent inelastic solids, Computational mechanics 12, 277 (1993)
[38] N. Moës, J. Dolbow, and T. Belytschko, A finite element method for crack growth without remeshing, *International journal for numerical methods in engineering* 46, 131 (1999).
[39] T. Belytschko and T. Black, Elastic crack growth in finite elements with minimal remeshing, *International journal for numerical methods in engineering* 45, 601 (1999).
[40] ABAQUS Theory Manual. 4.5.2 Damaged plasticity model for concrete and other quasi-brittle materials, *ABAQUS software manual*
[41] Groningen Earthquakes - Structural Upgrading report. Modelling prediction and analysis TUD-COMP-0b